Discrete Optimal Couple Tracking: a control scheme for electrical-tuning of strong coupling piezoelectric energy harvesters

Adrien Morel, Gaël Pillonnet, David Gibus, Adrien Badel

Discrete Optimal Couple Tracking: a control scheme for electrical-tuning of strong coupling piezoelectric energy harvesters

Adrien Morel[*a], Gaël Pillonnet[b], David Gibus[a], Adrien Badel[a]

[a]Univ. Savoie Mont Blanc, SYMME, 74000 Annecy, France
[b]Univ. Grenoble Alpes, CEA LETI, 38000 Grenoble, France

Abstract

In order to track the maximum power point of piezoelectric energy harvesters, an effective approach consists in designing interfaces able to electrically tune the harvester dynamics. Such interface should exhibit – at least – two tunable parameters in order to independently optimize the harvester damping and resonant frequency, i.e., an electromechanical impedance matching of the real and imaginary parts of the electrical load. In order to optimize and control these two parameters, it is necessary to implement two control loops that simultaneously impact the harvester dynamics. Furthermore, these loops should combine quick convergence time with low-power consumption in order to react sufficiently fast to compensate for any shift in the vibration frequency and to consume only a small portion of the harvested power. In this paper, we propose a control-law based on the successive evaluation of couples of parameters in order to select the optimal one. First, we determine analytically the expression of a set of optimal couples valid for any two-parameters electrical interfaces. Thereafter, we prove that only a few well-chosen couples of parameters are sufficient to maximize the power on a large frequency band. The proposed methodology has been experimentally verified on a tunable interface, the short-circuit synchronous electric charge extraction. Combined with a strongly coupled piezoelectric energy harvester, we have been able to maintain the harvested power close to the maximal achievable power (i.e., >70% of the maximal achievable power) on a 20 Hz frequency band, with only five couples of parameters. Such approach allows to substitute a multi-parameters convergence algorithm by a single-couple of parameters convergence algorithm, greatly simplifying the algorithm and reducing its convergence time.

Keywords: Piezoelectricity; Vibration energy harvesting; Nonlinear electronics; Discrete Maximum Power Point Tracking; Predictive model; Gradient algorithm; Frequency tuning; Broadband

Introduction

Energy harvesting has been widely investigated as a way to replace batteries for powering small electronic devices such as sensors nodes and wake-up radios [1]. In close environments, where solar radiations and thermal gradients are weak, vibration energy harvesters constitute a promising solution [2]. Among the various mechanical-to-electrical transduction mechanisms, piezoelectricity offers a good trade-off between compacity, power, and simplicity [3]. Most piezoelectric energy harvesters (PEH) are made of resonant structures that maximize the harvested power when the vibration frequency matches the PEH resonant frequency [4]. However, in many environments, the frequency of the vibrations varies with time, leading to poor performances when it shifts away from the PEH resonant frequency [5]. In order to enlarge the frequency bandwidth of PEH, several approaches and techniques have been proposed in the literature [6]. For instance, some researchers proposed to purposely bring nonlinearities into the behaviors of PEH in order to enhance their frequency bandwidth [7], but such nonlinear approach may lead to complicated behaviors that are amplitude- and orbit-dependent [8, 9]. Another approach consists in adapting in real-time the dynamics of

[*]Corresponding author, E-mail address: adrien.morel@univ-smb.fr

the PEH and to track the shifts of vibration frequency in order to always operate at resonance. Such approach can be implemented with many frequency tuning mechanisms, such as tunable magnets [10], screws or springs [11]. One of them consists in the electrical adjustment of the PEH resonant frequency and damping using tunable interface circuits (which can be seen as an electromechanical impedance matching) [12]. Such electrical tuning allows the elaboration of compact self-powered harvesting solutions that can adapt their own dynamics to the environment. However, the control of the electrical interface remains an important challenge that need to be tackled. Such approach requires the optimization of, at least, two electrical parameters in order to simultaneously tune the resonant frequency and damping and reach the PEH maximum power point (MPP)[1]. Furthermore, these parameters have to converge toward their optimal values in a minimal time and with a small power consumption.

Multi-parameters electrical interfaces that can tune the PEH resonant frequency and enlarge the harvesting bandwidth have been widely investigated in the last decade, as illustrated in Table 1. The first electrical tuning interfaces have been proposed by Wu et al. [13] and Liao et al. [14] and rely on the adjustment of a capacitive banks connected to the PEH. Such approach has been implemented by Bouhadjar et al. in 2014 with a capacitively-tuned full-bridge rectifier [15]. In 2014, Badel and Lefeuvre proposed the frequency-tuning synchronized electric charge extraction (FTSECE) [16]. FTSECE is a non-linear interface that allows the tuning of the resonant frequency and electrical damping by mean of a fine control of the phase-shift of the energy harvesting events and of the voltage inversion ratio. Such technique has been experimentally validated by Brenes et al. [17] and allows a significant gain in term of power and bandwidth, compared to a passive approach. Many other tunable interfaces such as the short-circuit SECE (SCSECE) that we proposed [18] and the phase-shift synchronized switch harvesting on inductor (PS-SSHI) proposed by Hsieh et al. [19] have been developed in the last few years as interesting alternatives to the FTSECE.

In order to maximize the harvesting power on a large frequency band, the aforementioned interfaces rely on the adjustment of two electrical parameters (e.g., a capacitive bank, the phase-shift of the energy harvesting event, or the duration of a short-circuit sequence). In most papers, these parameters have been tuned manually, in order to experimentally validate the basic principle of the tunable interface without any application-ready implementation [17, 18]. However, the design of an automated control of these parameters is not easy: it has to combine low-power consumption (i.e., in the µW range) with a fast convergence (ms – s convergence, depending on the application) of multiple electrical parameters (usually two parameters to optimize both the damping and the resonant frequency of the harvester). Among the literature, only a few papers tackle the need of an automated control. [20] proposes to realize such control with a low-power (≈1 µW) perturb & observe algorithm (for a single parameter interface). However, the convergence time of the algorithm (around 15-20s) might be too slow for many applications, and this algorithm might get trapped in local power maxima, hindering the potential of the tunable interface (Fig.1.a). In [21], Cai and Manoli proposed to realize such control using a look-up table, with pre-defined couples of parameters (depending on the detected vibration frequency). Such control, because of its relative simplicity, allows to combine low-power consumption (≈1 µW) with quasi-instantaneous convergence time (only depending on the electronics sensing the vibration frequency). However, the choice of the pre-defined couples of parameters is not explained in the paper, and is crucial in order to design such simple low-power fast-convergence algorithm.

In this paper, we propose a generic methodology in order to determine a minimal set of couples to maintain a harvested power larger than a targeted percentage of the achievable power on the largest possible frequency bandwidth, for any two-tuning electrical interfaces (Fig.1.b). The first section reminds the electromechanical model of linear piezoelectric energy harvesters as well as the impact of the electrical interface on the harvester dynamics, and proves the need of multi-parameter control of tunable electrical interfaces. The second section presents the generic analytical derivation of the optimal couples for any tunable interface. The third section proposes to analyze the impact of the number of couples on the harvester power-frequency response and on the convergence time of the tunable parameters. Finally, the last section provides an experimental validation

[1] Indeed, as shown in Table 1, a single tuning interface does not allow independent adjustment of the PEH resonant frequency and of the optimal damping, meaning that the electromechanical impedance matching conditions cannot be met for a whole range of vibration frequencies. In the one hand, multiple tuning interfaces allow to adjust independently the real and imaginary part of the load, meaning that the PEH resonant frequency and PEH damping can be optimized independently.

of the proposed methodology on the SCSECE, a two-tuning electrical interface. This experimental validation, while prototyped on a laptop and not being self-powered, validates the proposed methodology and paves the way toward low-power algorithms for PEH frequency tuning.

Table 1 – Adding tunability to the electrical interface to maximize the harvested power

Number of tuning	Examples of electrical interfaces	Type of matching	Reach power limit?	Power-frequency response	References
No tuning	SECE, OSECE, etc.	No matching	No (except for a given $k_m^2 Q$)	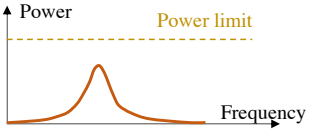	[22] [23]
Single tuning	Tunable SECE, Phase-shift SECE, N-SECE, etc.	Resistive-Reactive dependent matching	Yes (for one or two vibration frequencies)	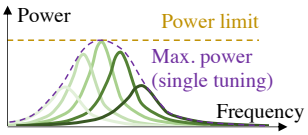	[24] [25] [26]
Multiple tuning	Tunable cap. bank, FTSECE, SCSECE, PS-SSHI	Electromechanical impedance matching	Yes (for a full range of vibration frequencies if $k_m^2 Q$ is large enough)	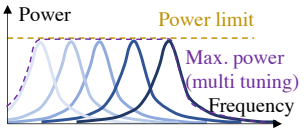	[15] [17] [18] [19]

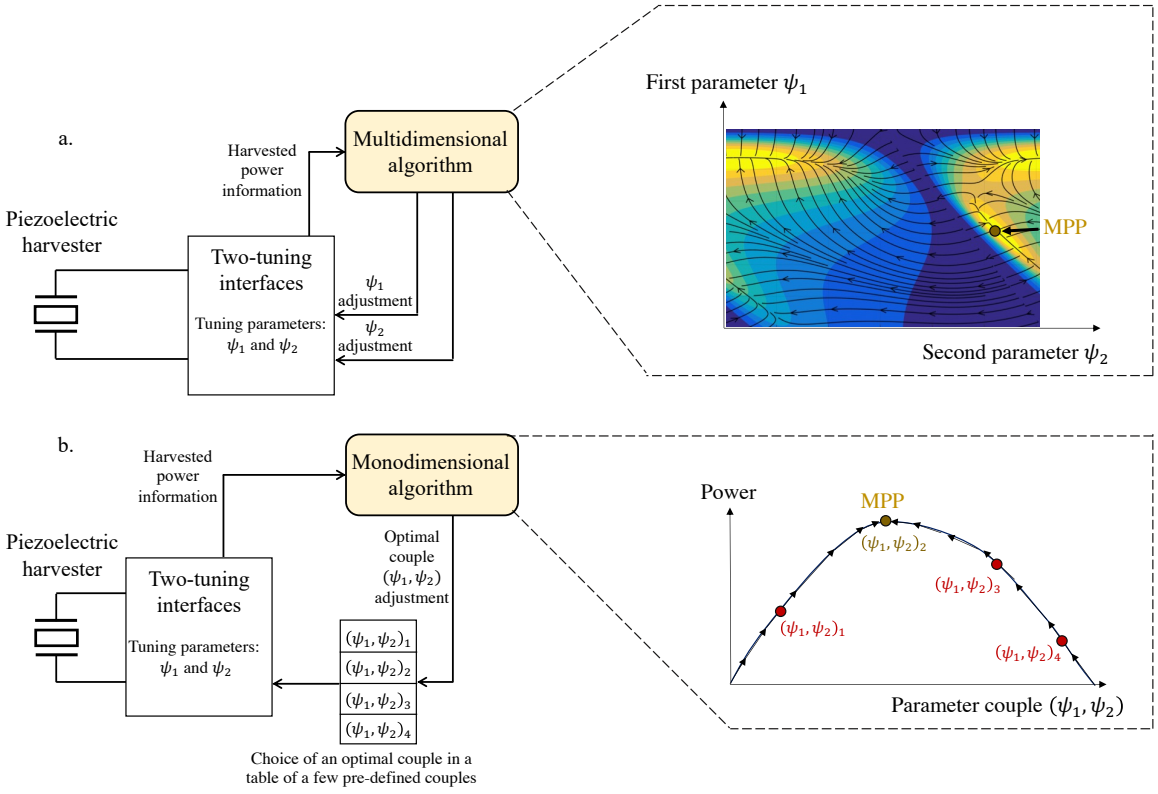

Figure 1. (a) Multi-parameter optimization by mean of a multi-dimensional algorithm and (b) proposed approach based on couples of parameter optimization by mean of a single mono-dimensional algorithm.

Electromechanical model of the energy harvester

In the literature, most linear piezoelectric energy harvesters (PEH) are made of piezoelectric plates bonded on a mechanical resonator (e.g., a cantilever beam). Under a sinusoidal vibration, the resonator starts to oscillate, and the piezoelectric material under strain generates electrical charges that can be collected by an electrical interface. Such single degree of freedom (SDoF) system is illustrated by Fig.2.a, with M being the inertial mass of the resonator, K being its stiffness, and D being the damping factor [4]. The electromechanical equations modeling the dynamic mass displacement x, the current flowing in the electrical interface i_p and the voltage across the piezoelectric element v_p can be written as (1).

$$\begin{cases} M\ddot{x}(t) + D\dot{x}(t) + Kx(t) + \alpha v_p(t) = -B_f\ddot{y}(t) \\ i_p(t) = \alpha\dot{x}(t) - C_p\dot{v_p}(t) \end{cases} \quad (1)$$

with $\ddot{y} = \gamma$ the ambient acceleration, and B_f the forcing term [27]. C_p is the piezoelectric material capacitance, and α is the force factor between the mechanical part and the electrical part of the PEH. This electromechanical model remains accurate as long as the strain in the piezoelectric material remains in the linear region, that the vibration frequency is close to the resonant frequency of the harvester, and that the dielectric losses are negligible [28].

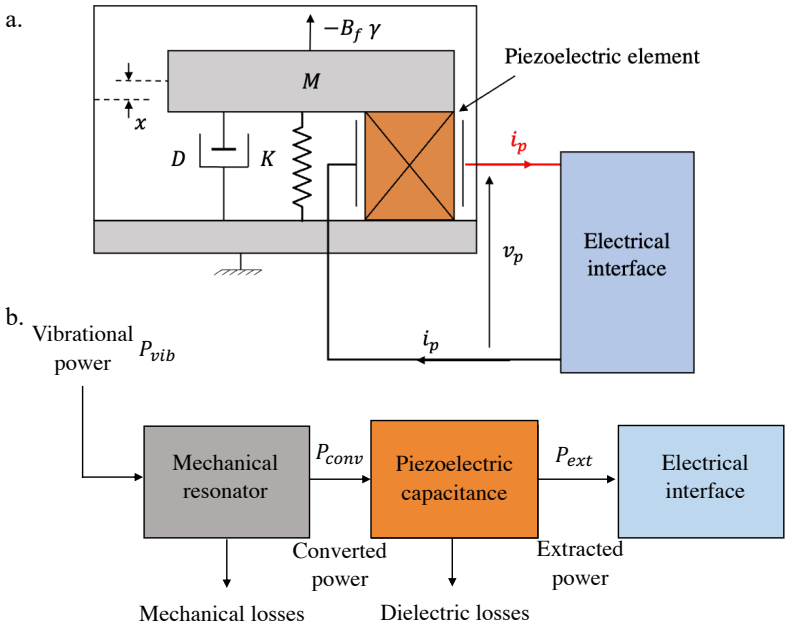

Figure 2. (a) Representation of a linear piezoelectric energy harvester and (b) power chain of the harvesting system.

We will consider that the external vibration is a monochromatic acceleration of amplitude γ_m whose pulsation ω might slowly vary with time. In this case, the mass displacement $x(t)$ can be approximated as a cosine wave of amplitude X_m, such that $\gamma = \gamma_m \cos(\omega t + \psi)$ and $x(t) = X_m \cos(\omega t)$, with ψ the phase difference between $\gamma(t)$ and $x(t)$. The piezoelectric voltage $v_p(t)$ is a periodic function and can be expressed as a Fourier series $v_p(t) = a_0 + \sum_{n=1}^{+\infty}[a_n \cos(n\omega t) + b_n \sin(n\omega t)]$, with a_n and b_n the n^{th} cosine and sine parameters of $v_p(t)$ Fourier series. Due to the filtering effect of the mechanical resonator (first equation of (1)), the higher frequency components of $v_p(t)$ share a negligible impact on the harvester dynamics (first harmonic assumption [28]). Hence, in order to compute the influence of the electrical interface on the PEH dynamics, only the fundamental of the piezoelectric voltage $v_p|_1$ has to be determined. As detailed in [17] and [28], $v_p|_1$ can be expressed as an in-phase and out-of-phase components with the mechanical displacement:

$$v_p|_1(t) = \frac{\alpha}{C_p}\left[\varepsilon_K(\psi_1,\psi_2)\, x(t) + \frac{\varepsilon_D(\psi_1,\psi_2)}{\omega}\frac{dx}{dt}(t)\right] \tag{2}$$

with $\varepsilon_D(\psi_1,\psi_2) = -\frac{b_1 C_p}{\alpha X_m}$ and $\varepsilon_K(\psi_1,\psi_2) = \frac{a_1 C_p}{\alpha X_m}$ the dimensionless electrically-induced damping and stiffness, respectively, and ψ_1 and ψ_2 two electrically-adjustable parameters (i.e., the frequency of the harvesting events [26], the angular phase of the harvesting events [25], the voltage inversion ratio [24], etc.) that can be tuned in order to control the electrical damping and stiffness. Combining (2) with the first equation of (1) yields (3).

$$\frac{1}{\omega_0^2}\frac{d^2x}{dt^2}(t) + \left[\frac{1}{Q\omega_0} + \frac{k_m^2\varepsilon_D(\psi_1,\psi_2)}{\omega}\right]\frac{dx}{dt}(t) + \left[1 + k_m^2\varepsilon_K(\psi_1,\psi_2)\right] x(t) = -\frac{\gamma(t)}{\omega_0^2}\frac{B_f}{M} \tag{3}$$

with $\omega_0 = \sqrt{M/K}$, $Q = \sqrt{KM}/D$ and $k_m^2 = \alpha^2/\left(KC_p\right)$ being the short-circuit resonance pulsation, the mechanical quality factor and the expedient electromechanical coupling of the PEH, respectively. (3) proves that the electrical interface has both an impact on the damping of the PEH (ε_D) and on its resonance frequency (ε_K). The analysis of (3) in the frequency domain leads to the expressions of the mechanical displacement $\underline{x}$ and the harvested power P_{ext}.

$$\underline{x} = \frac{-\underline{\gamma}/\omega_0^2}{[1 - \Omega^2 + k_m^2\varepsilon_K(\psi_1,\psi_2)] + j[\Omega/Q + k_m^2\varepsilon_D(\psi_1,\psi_2)]} \tag{4}$$

$$P_{ext} = P_{lim}\frac{4\ k_m^2\ \varepsilon_D\ \Omega/Q}{[1 - \Omega^2 + k_m^2\varepsilon_K(\psi_1,\psi_2)]^2 + [\Omega/Q + k_m^2\varepsilon_D(\psi_1,\psi_2)]^2} \tag{5}$$

with $P_{lim} = \left(B_f\gamma^2 Q\right)/(8\ \omega_0\ M)$ the maximum power that can be harvested with a linear PEH, as proved in [28], and $\Omega = \omega/\omega_0$ the normalized vibration frequency. (5) demonstrates that the power-frequency response of any linear PEH can be adjusted using an electrical interface. The normalized power $P_{nor} \in [0,1]$ is expressed by (6).

$$P_{nor} = \frac{P_{ext}}{P_{lim}} = \frac{4\ k_m^2\ \varepsilon_D\ \Omega/Q}{[1 - \Omega^2 + k_m^2\varepsilon_K(\psi_1,\psi_2)]^2 + [\Omega/Q + k_m^2\varepsilon_D(\psi_1,\psi_2)]^2} \tag{6}$$

It is possible to harvest the power limit P_{lim} ($P_{nor} = 1$) for any vibration frequency and for any PEH characteristics (k_m^2, Q) as long as the electrical interface respects the impedance matching conditions given by (7) [27].

$$\begin{cases} \varepsilon_D^{P_{lim}} = \dfrac{\Omega}{Q\ k_m^2} \\ \varepsilon_K^{P_{lim}} = \dfrac{1 - \Omega^2}{k_m^2} \end{cases} \tag{7}$$

$\varepsilon_D^{P_{lim}}$ and $\varepsilon_K^{P_{lim}}$ are the values of ε_D and ε_K that allow to harvest the power limit, P_{lim}. Tunable electrical interfaces have been recently developed in order to realize such electromechanical impedance matching, and enlarge the harvested power of PEH on large frequency ranges [16], [18]. Such harvesting interfaces require the use of multidimensional control to adjust the values of (ψ_1,ψ_2) and $(\varepsilon_D,\varepsilon_K)$ to respect the matching conditions given by (7). In this article, we propose a control methodology in order to replace the multidimensional control by a monodimensional control that can ease the convergence of (ψ_1,ψ_2), save power, and reduce the overall complexity of the electrical interface.

Principle of the discrete optimal couple tracking

The proposed scheme, named discrete optimal couple tracking (DOCT), consists in pre-determining the couples of electrically-controllable parameters (ψ_1, ψ_2) that maximize the robustness of the harvested power on a pre-defined frequency band $[\Omega_{min}, \Omega_{max}]$, in order to implement a monodimensional gradient algorithm that chooses the best parameters couple among the pre-determined ones. First, we propose to determine the optimal couples $(\varepsilon_D, \varepsilon_K)$ maximizing the robustness of the harvested power on $[\Omega_{min}, \Omega_{max}]$. Then, the optimal couples (ψ_1, ψ_2) can be found using the interface-dependent relation between (ψ_1, ψ_2) and $(\varepsilon_D, \varepsilon_K)$.

From (6), the resonant frequency of the system (i.e., the vibration frequency that maximizes the PEH power-frequency response) can be adjusted with ε_K, while the damping of the system can be adjusted with ε_D. Thus, if we define an electrical interface that can emulate a number $N_c \in \mathbb{N}^*$ of couples $(\varepsilon_{D,n_c}, \varepsilon_{K,n_c})$ (with $n_c \in [1, N_c]$ representing the index of the considered couple of electrical influences), this interface can be associated with a number N_c of power-frequency responses. For example, the power-frequency responses of an electrical interface capable of emulating three unbalanced[2] couples $(\varepsilon_{D,1}, \varepsilon_{K,1})$, $(\varepsilon_{D,2}, \varepsilon_{K,2})$ and $(\varepsilon_{D,3}, \varepsilon_{K,3})$ is illustrated by Fig.3.a.

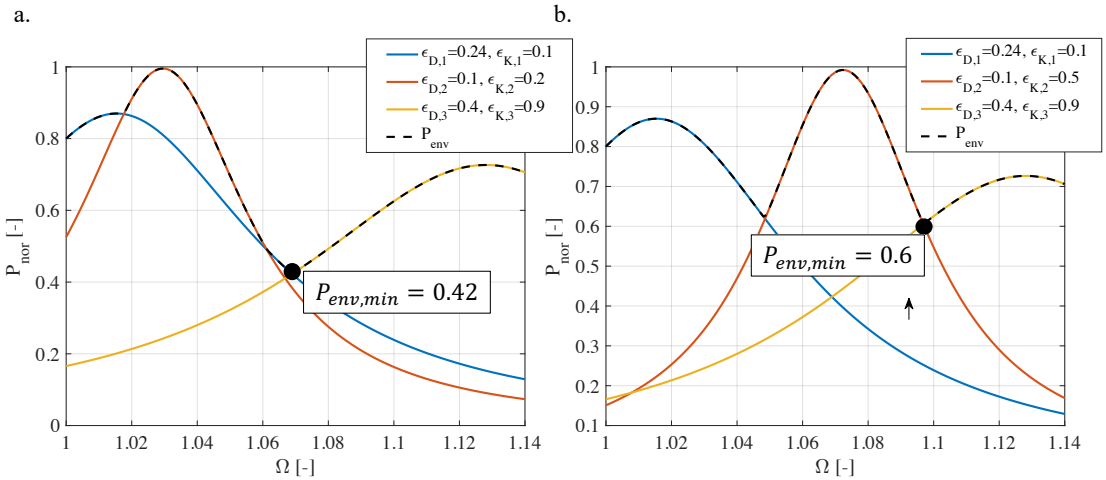

Figure 3. Power envelopes of a PEH with unbalanced couples: (a) $P_{env,min} = 0.42$ and (b) $P_{env,min} = 0.6$, with $\Omega_{min} = 1$, $\Omega_{max} = 1.14$ and a PEH exhibiting $k_m^2 = 0.3$ and $Q = 30$.

The maximum power achievable power for any frequencies with such interface will be called P_{env}, the power envelope, and is represented by a black dashed line in Fig.3. This envelope is defined mathematically by (8).

$$P_{env}(\Omega) = \max\{P_{nor}(\Omega, (\varepsilon_{D,n_c}, \varepsilon_{K,n_c})); n_c \in [1, N_c]\} \tag{8}$$

In order to maximize the robustness of the harvested power on a given frequency band $[\Omega_{min}, \Omega_{max}]$, we have to maximize the minimum of the power envelope on $[\Omega_{min}, \Omega_{max}]$. Such minimum is defined by (9).

$$P_{env,min} = \min\{P_{env}(\Omega); \Omega \in [\Omega_{min}, \Omega_{max}]\} \tag{9}$$

In Fig.3.a., the minimum of the power envelope P_{env} is relatively low ($P_{env,min} = 0.42$). In order to increase $P_{env,min}$, $\varepsilon_{K,2}$ can be increased, shifting the red power-frequency response on the right (higher resonance frequency), as shown in Fig.3.b. In this case, we can observe that $P_{env,min} = 0.6$.

[2] The couples are considered *unbalanced* if their power-frequency responses are not fairly distributed on the pre-defined frequency band $[\Omega_{min}, \Omega_{max}]$. Conversely, the couples are considered *balanced* if their power-frequency responses are fairly distributed on $[\Omega_{min}, \Omega_{max}]$.

Considering the linear behavior of the PEH, the minimum points $P_{env,min}$ always correspond to the intersections of two power-frequency responses. For example, in Fig. 3.a., $P_{env,min}$ corresponds to the intersection of the blue and yellow power-frequency responses. In Fig. 2 b), $P_{env,min}$ becomes the intersection of the red and yellow power-frequency responses. The optimal case that maximizes $P_{env,min}$ can be attained when the intersections of all the power-frequency responses share the same (maximized) value and are all fairly distributed on the frequency interval, as illustrated by Fig. 4 with $N_c = 3$ (balanced couples case).

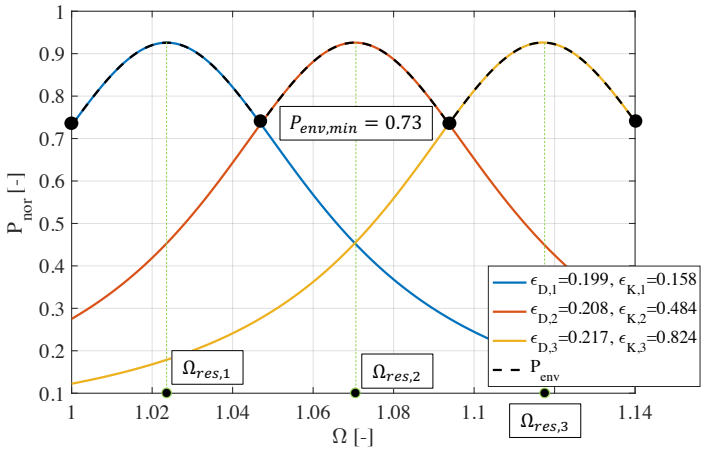

Figure 4. Optimization of the power envelope in order to maximize $P_{env,min}$ with three balanced couples, with $\Omega_{min} = 1, \Omega_{max} = 1.14$ and a PEH exhibiting $k_m^2 = 0.3$ and $Q = 30$.

Hence, in order to maximize $P_{env,min}$, the first condition is that the N_c resonant frequencies corresponding to the N_c power-frequency responses must be evenly spaced in $[\Omega_{min}, \Omega_{max}]$. This condition is expressed analytically by (10).

$$\forall n_c \in [1, N_c], \qquad \Omega_{res,n_c} = \Omega_{min} + \frac{(\Omega_{max} - \Omega_{min})}{2N_c}(2n_c - 1) \tag{10}$$

Combining (10) with the matching condition on ε_K expressed by (7) leads to (11).

$$\forall n_c \in [1, N_c], \qquad \varepsilon_{K,n_c} = \frac{\Omega_{res,n_c}^2 - 1}{k_m^2} = \frac{\left[\Omega_{min} + \frac{\Omega_{max} - \Omega_{min}}{2N_c}(2n_c - 1)\right]^2 - 1}{k_m^2} \tag{11}$$

If (11) is respected, the normalized frequencies Ω_0 that correspond to the minima of the power envelope are given by (12).

$$\Omega_{0,n_c} = \Omega_{min} + \frac{(\Omega_{max} - \Omega_{min})}{N_c} n_c \tag{12}$$

To maximize $P_{env,min}$, the second condition is to maximize the value of the power envelope when $\Omega = \Omega_{0,n_c}$ $\forall n_c \in [1, N_c]$. This condition is expressed analytically by (13).

$$\forall n_c \in [1, N_c], \quad \frac{\partial P_{nor}}{\partial \varepsilon_D}\Big|_{\Omega=\Omega_{0,n_c}, \varepsilon_K=\varepsilon_{K,n_c}} = 0 \tag{13}$$

Solving (13), we obtain the following condition on the N_c electrical damping ε_{D,n_c}:

$$\forall n_c \in [1, N_c], \quad \varepsilon_{D,n_c} = \frac{\sqrt{\left(1 - \Omega_{0,nc}^2 + k_m^2 \varepsilon_{K,n_c}\right)^2 + \frac{\Omega_{0,n_c}^2}{Q}}}{k_m^2} \tag{14}$$

Hence, the optimality conditions on the N_c discrete couples $\left(\varepsilon_{D,n_c}, \varepsilon_{K,n_c}\right)$ have been determined and are given by (11) and (14). The only parameters that are needed in order to find such optimal couples are the piezoelectric electromechanical coupling k_m^2 and Q. These two parameters can easily be found with an impedance analysis of the PEH, as shown in [16]. Note that none of the N_c optimal discrete couples $\left(\varepsilon_{D,n_c}, \varepsilon_{K,n_c}\right)$ are equal to $(\varepsilon_D^{Plim}, \varepsilon_K^{Plim})$ because the aim of DOCT is not to harvest the power limit on the whole frequency range of interest, but to harvest a power close to this power limit with a few optimal couples.

Critical coupling and $[\Omega_{min}, \Omega_{max}]$ for implementing the DOCT

Practically, the values of ε_D and ε_K are bounded and depend on the choice of the electrical interface. This mean that it might not be possible to fulfill the optimality conditions on ε_{K,n_c} and ε_{D,n_c} given by (11) and (14) if the values of $\max(\varepsilon_D)$ and $\max(\varepsilon_K)$ (with a given interface) are too small, or if k_m^2 is too small (meaning that the impact of the electrical interface does not allow to induce the optimal damping or stiffness). In order to ensure that (14) can be fulfilled for all N_c, $\max(\varepsilon_D)$ should be greater or equal to a limit value given by (15).

$$\max(\varepsilon_D) \geq \frac{\sqrt{\frac{(\Omega_{max} - \Omega_{min})^2}{4} + \frac{\Omega_{max}^2}{Q}}}{k_m^2} \tag{15}$$

If the case of a weakly coupled PEH, $\Omega_{max} \approx \Omega_{min} \approx 1$. Therefore, in this case, (15) becomes (16).

$$k_m^2 \geq \frac{1}{Q \max(\varepsilon_D)} = k_{m,c}^2 \tag{16}$$

This means that the PEH electromechanical coupling k_m^2 should be greater than $(Q \max(\varepsilon_D))^{-1}$ in order to implement the DOCT. $k_{m,c}^2 = (Q \max(\varepsilon_D))^{-1}$ is the critical coupling which separates weakly coupled PEH ($k_m^2 < k_{m,c}^2$) from strongly coupled PEH ($k_m^2 > k_{m,c}^2$), as defined in [29]. For instance, in the case of the SCSECE interface, $\max(\varepsilon_D) = 4/\pi$ [18]. To implement the DOCT with the SCSECE interface, the electromechanical coupling of the PEH should be greater than $\pi/(4Q)$. (16) is consistent with the definition of critical coupling and coupling state given in [29] and [30]. Indeed, [29] proves that such critical coupling depends on the choice of electrical interface and on the quality factor of the PEH.

In order to ensure that (11) is fulfilled, the pre-defined frequency band $[\Omega_{min}, \Omega_{max}]$ where the DOCT algorithm maximizes the harvested power should be chosen such that (17) is respected. (17) shows that the stronger the electromechanical coupling k_m^2, the larger the frequency band where the DOCT algorithm can be used.

$$\begin{cases} \Omega_{min} \geq \sqrt{1 + k_m^2 \min(\varepsilon_K)} \\ \Omega_{max} \leq \sqrt{1 + k_m^2 \max(\varepsilon_K)} \end{cases} \tag{17}$$

For instance, with a RC load ($\min(\varepsilon_K) = 0$, $\max(\varepsilon_K) = 1$ [18]), the maximum pre-defined frequency band is given by $[1, \sqrt{1 + k_m^2}]$. With a SCSECE interface ($\min(\varepsilon_K) = 1/2 - 2/\pi$, $\max(\varepsilon_K) = 1.6366$ [31]), the maximum pre-defined frequency band is given by $[\sqrt{1 + k_m^2(1/2 - 2/\pi)}, \sqrt{1 + 1.6366\, k_m^2}]$.

Number of couples: a trade-off between power and convergence time

Figure 5 shows the values of these optimal couples in the plane $(\varepsilon_D, \varepsilon_K)$ for various number of couples N_c, as well as the associated power-frequency responses. The black dotted line ($N_c \to \infty$) corresponds to the case where the number of couples is infinite, and matches the electromechanical impedance matching conditions given by (7) (which is, indeed, the solution to the continuous limit-case of the optimality problem studied in this paper).

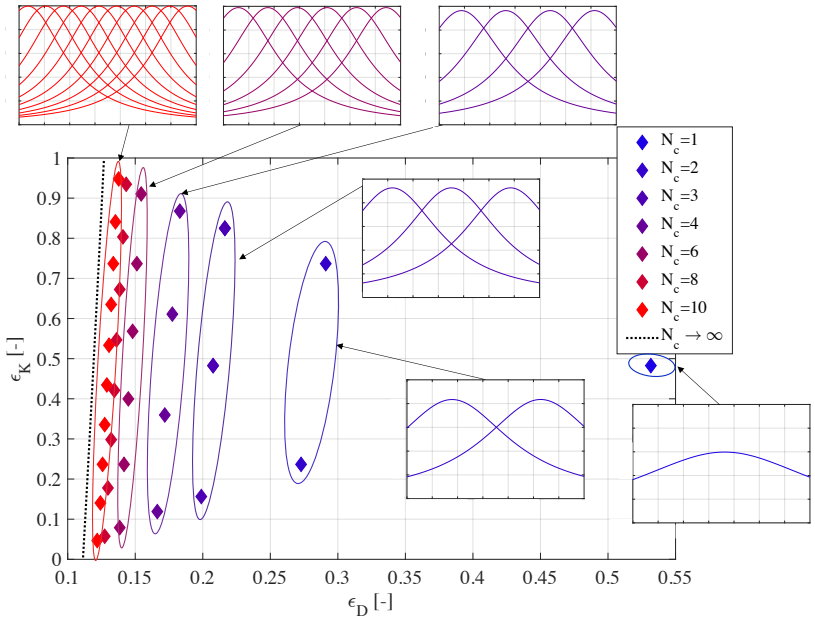

Figure 5. Values of the optimal couples $(\varepsilon_{D,n_c}, \varepsilon_{K,n_c})$ in the plane $(\varepsilon_D, \varepsilon_K)$ with various number of couples N_c with $\Omega_{min} = 1$, $\Omega_{max} = 1.14$ and a PEH exhibiting $k_m^2 = 0.3$ and $Q = 30$.

From Fig. 5, we can verify that a greater number of couples N_c leads to a greater $P_{env,min}$. If N_c is sufficiently large, $P_{env,min}$ gets close to 1 (corresponding to an extraction of the power limit P_{lim} on the whole frequency band). Interestingly, the values of the optimal couples $(\varepsilon_{D,n_c}, \varepsilon_{K,n_c})$ greatly vary with the number of these couples N_c[3], meaning that the optimal couples cannot be directly determined from the impedance matching theory and are not equal to $(\varepsilon_D^{P_{lim}}, \varepsilon_K^{P_{lim}})$ (7).

Figure 6.a shows the evolution of $P_{env,min}$ as a function of the number of couples N_c, for various piezoelectric energy harvesters ($k_m^2 Q$), with a fixed $Q = 30$. In in each case, Ω_{min} has been fixed to 1 and Ω_{max} has been fixed to $\sqrt{1 + k_m^2} = \sqrt{1.3}$, which correspond to the normalized short-circuit and open-circuit resonant frequencies of the PEH [27, 29]. Note that the results shown in Fig. 6.a remain sensibly the same with other values of Q, as long as the products $k_m^2 Q$ remain unchanged. With a greater $k_m^2 Q$, it becomes necessary to increase the number of couples N_c in order to maintain a large $P_{env,min}$. Indeed, if k_m^2 is increased, the frequency range $[\Omega_{min}, \Omega_{max}]$ where the PEH dynamics can be tuned becomes larger [31], leading to a decrease of $P_{env,min}$ for a given N_c. If Q is increased, the maximum harvested power increases (because P_{lim} grows linearly with Q [28]), but the bandwidth associated with each power-frequency response become smaller ($\propto 1/Q$) which also leads to a decrease of $P_{env,min}$ for a given N_c[4]. However, a large N_c leads to a slower algorithm convergence. The algorithm convergence time can be majored by considering an algorithm that tests every couple, maintain each of them during a specific duration, then select the optimal one (such as the one illustrated in Fig.7). In this case, the total time t_{conv} to find the optimal couple is given by the product of the number of couples with the time taken to converge to steady-state for a single couple. By considering that the PEH behaves as a second-order system, its settling time[5] in pseud-

[3] In other terms, $(\varepsilon_{D,n_c}, \varepsilon_{K,n_c})$ with $N_c = 2$ is not a subset of $(\varepsilon_{D,n_c}, \varepsilon_{K,n_c})$ with $N_c = 4$.

[4] Note that the absolute value of the minimum of the power envelope with a given N_c does not change with an increase of Q, but its normalized value $P_{env,min}$ relative to the achievable power, P_{lim}, decreases because P_{lim} grows linearly with Q.

[5] The settling time is "the time required for the response curve to reach and stay within a range of a certain percentage of the final value", as defined in [32].

periodic regime is given by $t_{set} = -\frac{2\,Q\,\ln\left(tol\sqrt{1-\frac{1}{4Q^2}}\right)}{\omega_0}$, with tol being the tolerance fraction that is the maximum percentage of error between the final value and the value obtained after a time t_{set}, as depicted in Fig.7. Therefore, t_{conv} can be evaluated as (18):

$$t_{conv} = -\frac{2\,Q\,N_c \ln\left(tol\sqrt{1-\frac{1}{4Q^2}}\right)}{\omega_0} \tag{18}$$

The number of periods before convergence, N_{period}, can thus be evaluated as:

$$N_{period} = -\frac{2\,Q\,N_c\,\Omega\,\ln\left(tol\sqrt{1-\frac{1}{4Q^2}}\right)}{2\pi} \tag{19}$$

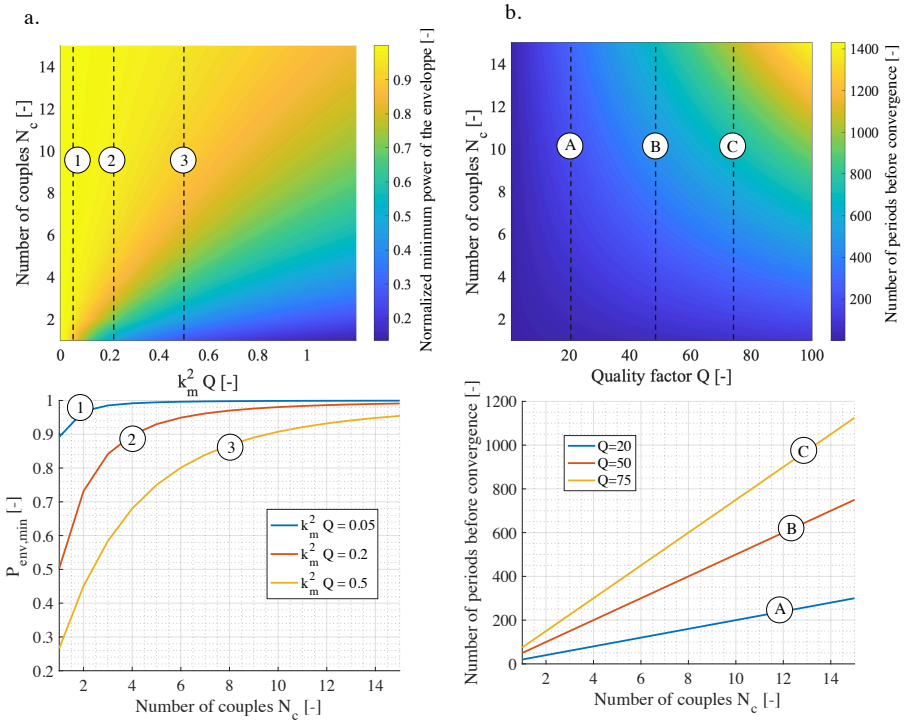

Figure 6. (a) $P_{env,min}$ as a function of the number of couples $(\varepsilon_D, \varepsilon_K)$ and of the product of the PEH electromechanical coupling and quality factor $k_m^2 Q$ (with $Q = 30$), and (b) Number of periods before convergence as a function of the number of couples $(\varepsilon_D, \varepsilon_K)$ and of the quality factor of the PEH Q, with $tol = 5\%$.

Figure 6.b shows the evolution of the number of periods before convergence, N_{period}, as a function of the quality factor of the PEH, Q, and the number of couples N_c. As shown in Fig.6.b, a larger number of couples as well as a larger Q tend to increase the time taken by the algorithm before its convergence. Therefore, there exists a trade-off between the time taken by the algorithm to converge and the minimum value of the power envelope, $P_{env,min}$. Depending on the application requirements and on the PEH characteristics, N_c should be chosen in order to obtain a sufficient power in a minimum convergence time.

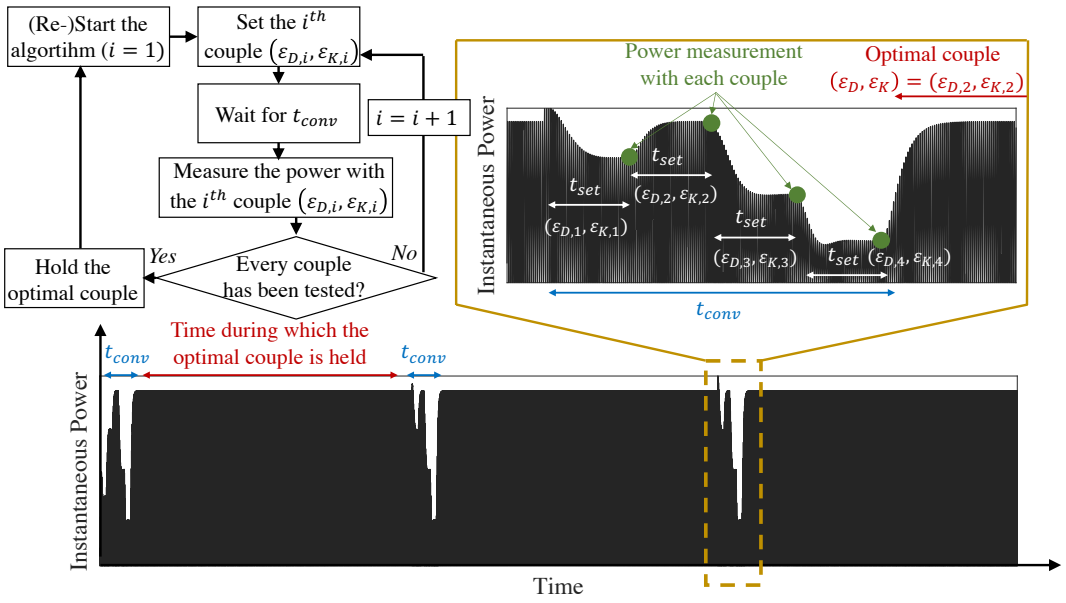

Figure 7. Illustration of the algorithm convergence after evaluating the harvested power for each couple of parameters (with $N_c = 4$)

Implementing the DOCT with a tunable electrical interface

Equations (11) and (14) give the optimal values of the electrical damping ε_D and stiffness ε_K for a given number of couples N_c. To find the optimal couples of electrical parameters (ψ_1, ψ_2), the interface-dependent relation between $(\varepsilon_D, \varepsilon_K)$ and (ψ_1, ψ_2) has to be known. Such relations are given in Table 2 for some tunable interfaces that have been proposed in the recent literature. Note that for each interface, the electrically-controllable parameters can be of different nature: for the SCSECE, ψ_1 represents the phase-shift between the displacement extremum and the harvesting event, and ψ_2 is the angular duration of a short-circuit sequence. For the FTSECE and the FT-OSECE, ψ_1 represents the voltage inversion ratio, and ψ_2 represents the phase-shift between the displacement extremum and the harvesting event. In the case of the RC load, ψ_1 represents the normalized resistive load $\psi_1 = R_{load} C_p \omega_0$ and ψ_2 represents the normalized capacitive load $\psi_2 = C_p/(C_p + C_{load})$.

Table 2 – Relations between the electrically-controllable parameters $(\boldsymbol{\psi_1}, \boldsymbol{\psi_2})$ and the electrical damping and stiffness $(\boldsymbol{\varepsilon_D}, \boldsymbol{\varepsilon_K})$ for some two-tuning interfaces in the literature.

Strategy	ε_D	ε_K	Ref.
Tunable RC load	$\frac{(\boldsymbol{\psi_1}\Omega)^2}{1-\boldsymbol{\psi_2}}\left[1+\left(\frac{\boldsymbol{\psi_1}\Omega}{1-\boldsymbol{\psi_2}}\right)^2\right]^{-1}$	$\boldsymbol{\psi_1}\Omega\left[1+\left(\frac{\boldsymbol{\psi_1}\Omega}{1-\boldsymbol{\psi_2}}\right)^2\right]^{-1}$	[13, 14]
FTSECE	$\frac{4}{\pi}\frac{1-\boldsymbol{\psi_1}}{1+\boldsymbol{\psi_1}}\cos^2(\boldsymbol{\psi_2})$	$1+\frac{2}{\pi}\frac{1-\boldsymbol{\psi_1}}{1+\boldsymbol{\psi_1}}\sin(2\boldsymbol{\psi_2})$	[17]
SCSECE	$\frac{[\cos(\boldsymbol{\psi_1})+\cos(\boldsymbol{\psi_1}+\boldsymbol{\psi_2})]^2}{\pi}$	$1-\frac{\boldsymbol{\psi_2}}{\pi}+\frac{\sin(2\boldsymbol{\psi_1}+2\boldsymbol{\psi_2})}{2\pi}+\sin\frac{(2\boldsymbol{\psi_1})}{2\pi}+2\frac{\cos(\boldsymbol{\psi_1}+\boldsymbol{\psi_2})\sin(\boldsymbol{\psi_1})}{\pi}$	[18]
FT-OSECE	$\frac{4}{\pi}\frac{1-\boldsymbol{\psi_1}}{1+\boldsymbol{\psi_1}}\cos^2(\boldsymbol{\psi_2})$	$1+\frac{2}{\pi}\frac{1-\boldsymbol{\psi_1}}{1+\boldsymbol{\psi_1}}\sin(2\boldsymbol{\psi_2})$	[33]

Some other tunable interfaces in the literature such as the PS-SSHI [19, 34] or the SC-SEH [35] have not been included in Table 2 because their expressions of ε_D and ε_K are too long. However, such expressions can be found in the associated references and can be used to apply the DOCT methodology to these interfaces as well.

From the expressions given in Table 2 and equations (11) and (14), it becomes possible to compute the optimal couples of electrically-controllable parameters (ψ_1, ψ_2) for any tunable interfaces.

Experimental validation

In order to validate the proposed methodology, we designed a custom strongly-coupled PEH which is shown in Fig. 8. This harvester is made of a steel cantilever beam (total volume: 60 mm^3), covered by two plates of PZN-PT single crystals. Two long profile masses (total volume: 375 mm^3) in steel are fixed to the harvester in order to decrease its resonance frequency and increase its power density [18]. The dimensions of this prototype are indicated in Fig. 8 and its measured characteristics are summarized in Table 3.

This custom harvester is fixed on an electromagnetic shaker powered by a power amplifier and vibrating at an acceleration of amplitude $\gamma_m = 0.3m.s^{-2}$.The displacement and speed of the inertial mass are sensed with a laser Doppler vibrometer, and the base acceleration is sensed using an accelerometer. The electrodes of the PEH are connected to a circuit on a breadboard that emulates the tunable SCSECE strategy. The whole experimental setup, illustrated in Fig. 9, is connected to a dSPACE control system that allows the real-time adjustment of the vibration frequency and of the tunable parameters (ψ_1, ψ_2) of the SCSECE interface, and store the voltage, displacement and acceleration waveforms in order to compute, for each set of parameters, the extracted power. Note that the proposed experimental setup allows to verify the validity of the DOCT methodology, but does not constitute a self-powered low-power implementation of a DOCT algorithm. However, we think that such low-power implementation is possible with a dedicated ASIC, as proved by recent realizations in the literature [20, 21].

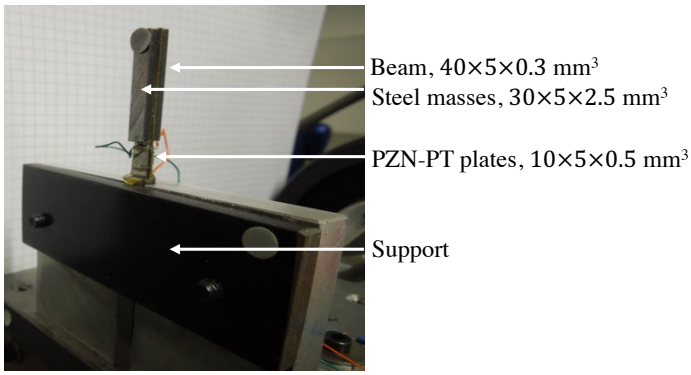

Figure 8. Custom strongly coupled piezoelectric energy harvester

Table 3 – Characteristics of the custom PMN-PT piezoelectric energy harvester

Parameter	Identified value	Unit
k_m^2	0.48	-
ω_0	595	rad/s
Q	20	-
C_p	1.22	nF
P_{lim} (for $\gamma_m = 0.3m.s^{-2}$)	6	µW

The optimal (ψ_1, ψ_2) are numerically found from equations (11) and (14) and from the electrical damping and stiffness expressions given in Table 2. These optimal (ψ_1, ψ_2) (corresponding to the phase-shift between the displacement extremum and the harvesting event, and the angular duration of a short-circuit sequence, respectively) are shown in Table 3.

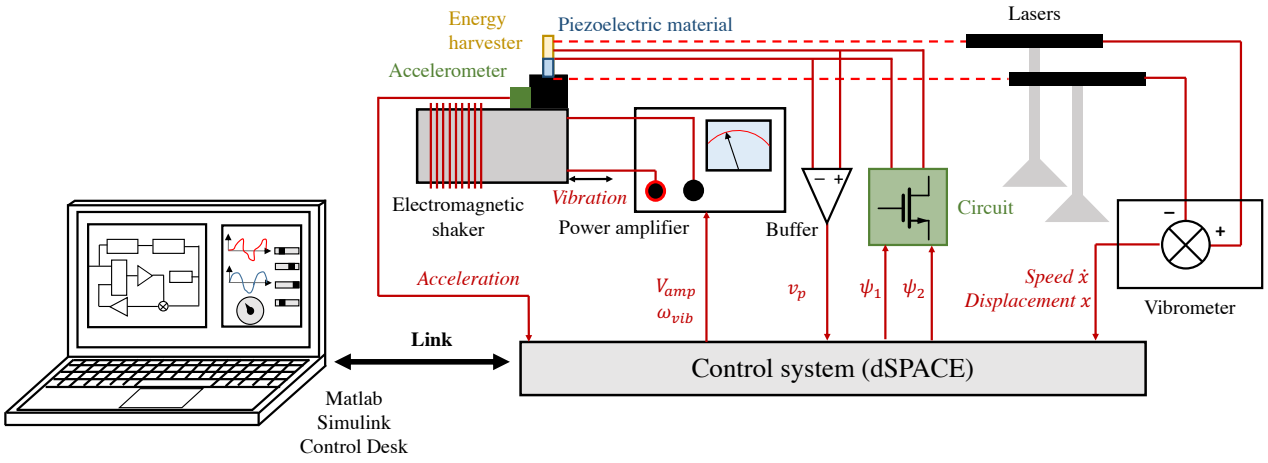

Figure 9. Experimental testbench that has been used in order to evaluate the proposed approach

Table 3 – Optimal couples of electrical parameters (ψ_1, ψ_2) for the SCSECE

	$N_c = 1$	$N_c = 3$			$N_c = 5$				
	$n_c = 1$	$n_c = 1$	$n_c = 2$	$n_c = 3$	$n_c = 1$	$n_c = 2$	$n_c = 3$	$n_c = 4$	$n_c = 5$
ε_{D,n_c}	0.540	0.194	0.207	0.220	0.143	0.149	0.155	0.161	0.167
ε_{K,n_c}	0.476	0.153	0.476	0.820	0.091	0.276	0.476	0.680	0.891
$\psi_{1,opt}$	164°	94.6°	112°	33.3°	139°	177°	18.0°	31.5°	42.3°
$\psi_{2,opt}$	86.4°	39.6°	4.50°	57.6°	136°	112°	87.3°	66.6°	47.7°

We have experimentally fixed the values of ψ_1 and ψ_2 to the values indicated in Table 3. Then, for 38 vibration frequencies chosen between 95 Hz ($\Omega = 1.00$) and 116 Hz ($\Omega = 1.22$), we have acquired the voltage waveforms. Thereafter, the extracted power from the piezoelectric energy harvester is determined by calculating $P_{ext} = C_p\, f\, v_{harv}^2$ [18] with f the vibration frequency and v_{harv} the piezoelectric voltage right before the energy extraction. The measured extracted powers as a function of the vibration frequency (normalized by the limit power P_{lim}) for a single couple of parameters ($N_c = 1$), three couples of parameters ($N_c = 3$), and five couples of parameters ($N_c = 5$) are shown in Fig.10.

Discussions

As shown in Fig.10, the theoretical predictions are in good agreement with the experimental data that have been measured with the automated testbench. The differences between experimental data and theoretical predictions may come from some mechanical and piezoelectric nonlinearities that have not been considered in the linear model given by (1), and from the influence of the higher resonant modes of the cantilever beam that have been neglected in our analysis. As shown in Fig.10, the minimum power envelope $P_{min,env}$ is equal to 0.35 for a single couple of parameters, 0.63 for three parameters, and 0.73 for five parameters. This shows, for instance, that more than 63% of the power limit P_{lim} can be harvested on a frequency band as large as 22% of the PEH short-circuit resonant frequency with only three well-chosen couples of electrical parameters (that have been determined with the DOCT methodology).

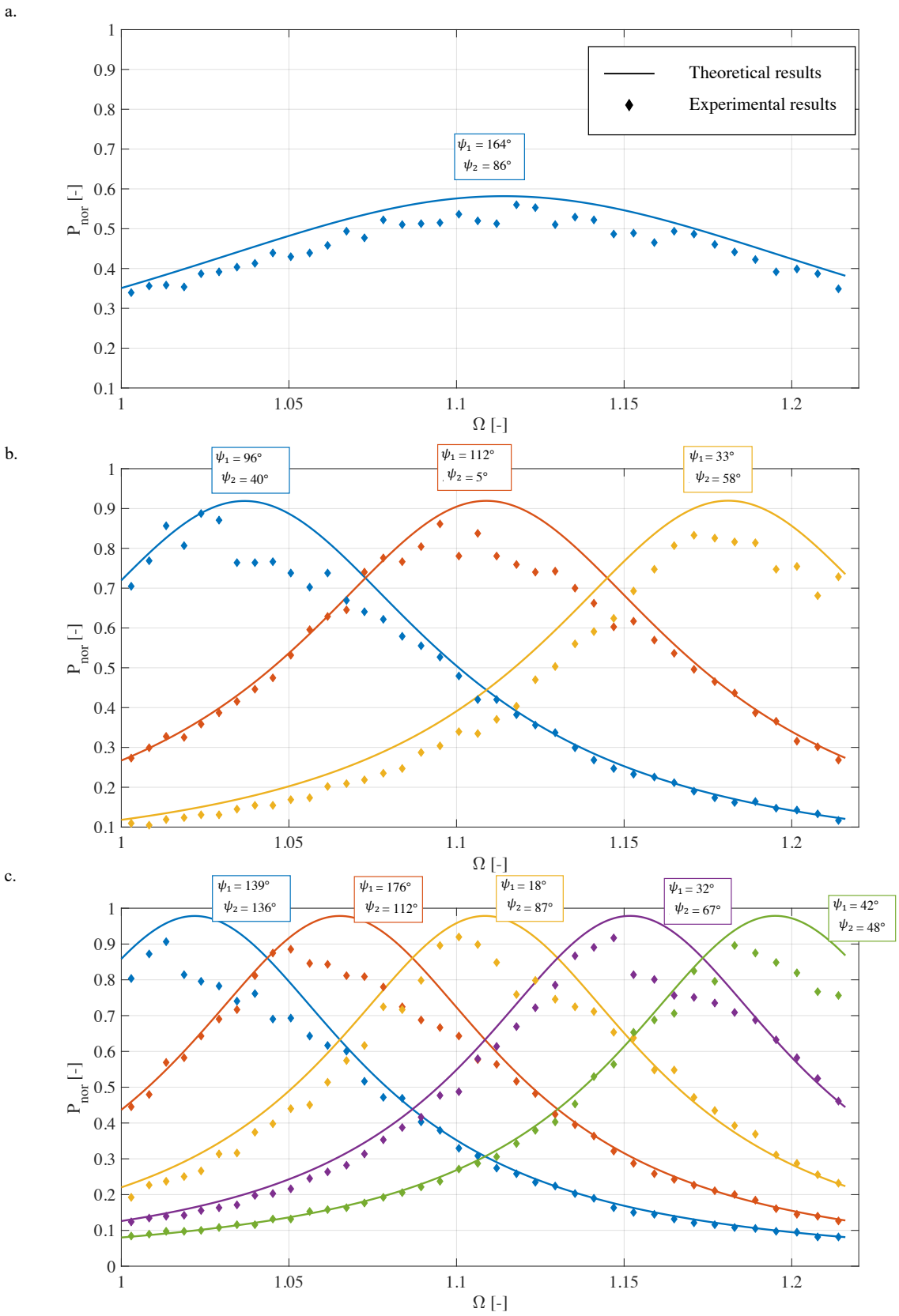

Figure 10. Optimal couples for $\Omega \in [1, 1.22]$ for the SCSECE strategy and with (a) $N_c = 1$, (b) $N_c = 3$ and (c) $N_c = 5$. The lines are the predicted power from (6) and the expressions of the electrical damping and stiffness given in Table 2. The diamonds correspond to the measured power on the experimental PEH shown in Fig.8 and using the testbench shown in Fig.9.

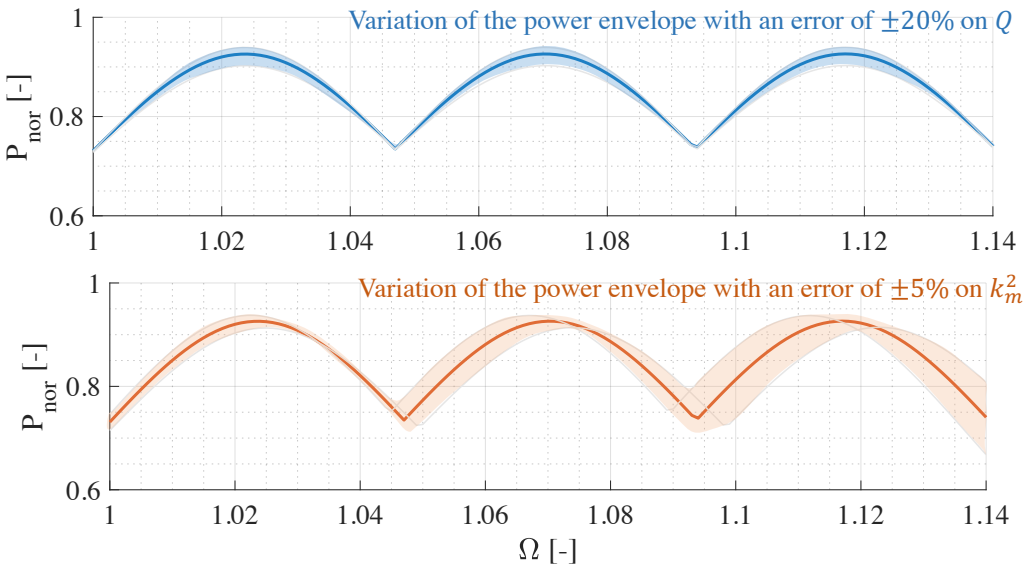

Figure 11. Simulation of the variation of the power envelopes with an error of ±20% on Q and an error of ±5% on k_m^2, with $k_m^2 = 0.3$, $Q = 30$ and $N_c = 3$.

While the proposed approach requires the characterization of the PEH (because it is necessary to know its k_m^2 and Q to find the optimal couples), Fig.11 shows that an error on these values (or a derive of these values because of aging or temperature variations) does not impact much the power envelope obtained with the optimal couples. Indeed, an error of 20% on Q decreases the minimum of the power envelope by less than $0.01P_{lim}$. An error of 5% on k_m^2 leads to a decrease of about $0.05P_{lim}$.

Note that the proposed methodology, DOCT algorithm, as well as the sensitivity analysis (Fig.11) could be applied to any electrical interface that exhibits, at least, two tunable parameters. The only condition on the electrical interface is that its electrically-induced damping and stiffness (with a given set of tunable parameters) should meet the optimality criteria given by (11) and (14). The convergence times of any electrical interface associated with the DOCT algorithm, are, in theory, identical and can be estimated with (19). As a matter of example, a DOCT-based algorithm (with the five couples of optimal parameters shown in Table 3) has been simulated on Simulink, with a model of the SCSECE interface and a model of the PEH shown in Fig.8. Figure 12 shows the piezoelectric voltage waveforms when the normalized vibration frequency shifts from $\Omega = 1.16$ to $\Omega = 1.05$. As shown in Fig.12, because of this frequency shift, the voltage (and the power) drastically decreases when $t = 8s$. Around $t = 10s$, all the five optimal couples (ψ_1, ψ_2) are successively tested (in approximately 1 second, as estimated by (19)) and the optimal couple is kept and stored in the system.

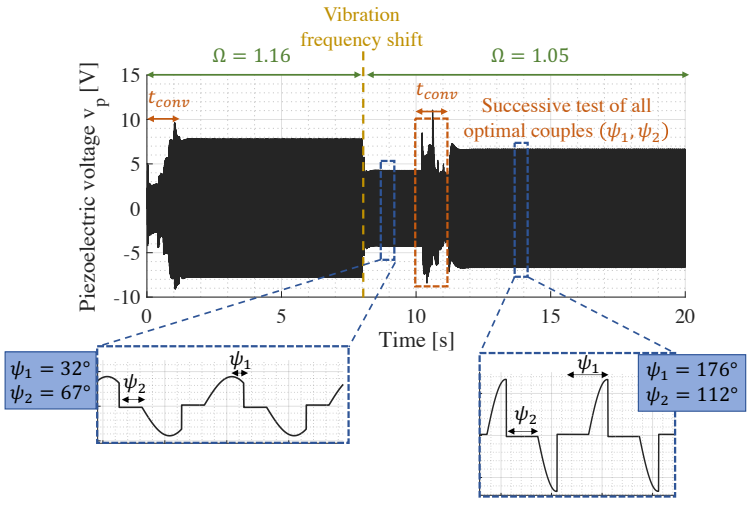

Figure 12. Simulation of a DOCT-based algorithm convergence with the PEH shown in Fig.8 and the SCSECE interface ($k_m^2 = 0.48$, $Q = 20$ and $N_c = 5$).

Such approach enables the design of low-power and fast algorithms that could determine, depending on the vibration frequency, which couple among the three optimal ones should be chosen. The convergence time of such algorithms could be much smaller than traditional approaches based on multidimensional gradients between a set of hundreds of parameters values. For instance, the time taken to test every couple of parameters and find the optimal one with the PEH shown in Fig.8 and for a single couple of parameters, three couples of parameters and five couples of parameters, are 0.2, 0.6 and 1 second, respectively. In comparison, the time taken by a gradient algorithm (with only a single tuning parameter) [20] is around 15 to 20 seconds. Such quick convergence allows the fast adjustment of the resonant frequency, enabling the compensation of aging and temperature effects that might induce resonant frequency shifts. Another notable advantage of DOCT-based algorithms is their intrinsic stability: the optimal couple can be found with an exhaustive comparison of the power obtained with each couple, or with a derivative-free method such as a dichotomous search.

Conclusion

In this paper, we introduce a methodology to choose a few optimal couples of tunable parameters that maximize the harvested power of a given harvester on a large frequency band. The generic expression of the optimal couples has been derived analytically, and is valid for any two-tuning electrical interfaces. We showed that in most case, only three to five couples are enough to scavenge a power relatively close to the the available power on the largest possible frequency band. The proposed methodology has been verified experimentally on a tunable interface, the SCSECE. Combined with a strongly coupled piezoelectric energy harvester, we have been able to harvest more than 70% of the available power on a 20Hz frequency band (for a resonant frequency of 95Hz), with only five couples of parameters. Such methodology paves the way toward simple algorithms combining low-power consumption with fast-convergence.

References

[1] M.T. Penella, J. Albesa, and M. Gasulla, “Powering wireless sensor nodes: Primary batteries versus energy harvesting”, *International Instrumentation and Measurement Technology Conference,* Singapore, 5-7 May 2009.
[2] J. Siang, M.H. Lim, and M. Salman Leong, “Review of vibration-based energy harvesting technology: Mechanism and architectural approach”, *International Journal of Energy Research*, pp. 1-28, 2018.
[3] S. Roundy, E. S. Leland, J. Baker, E. Carleton, E. Reilly, E. Lai, B. Otis, J. M. Rabaey, P. K. Wright, and V. Sundararajan, “Improving power output for vibration-based energy scavengers,” *IEEE Pervasive Computing*, vol. 4, no. 1, pp. 28–36, Jan. 2005.
[4] C. B. Williams and R. B. Yates, "Analysis Of A Micro-electric Generator For Microsystems," *Proceedings of the International Solid-State Sensors and Actuators Conference - TRANSDUCERS '95*, pp. 369-372, 1995.
[5] T. Yildirim, M. H. Ghayesh, W. Li, G. Alici, “A review on performance enhancement techniques for ambient vibration energy harvesters”, *Renewable and Sustainable Energy Reviews*, **71**, pp. 435-449, 2017.
[6] J. Twiefel, H. Westermann, “Survey on broadband techniques for vibration energy harvesting”, *Journal of intelligent material systems and structures,* **24**, 11, pp. 1291-1302, 2013.
[7] F. Cottone, H. Vocca, and L. Gammaitoni, “Nonlinear Energy Harvesting”, *Physical Review Letters*, **102**, 080601, 2009.
[8] T. Huguet, A. Badel, O. Druet, M. Lallart, “Drastic bandwidth enhancement of bistable energy harvesters: Study of subharmonic behaviors and their stability robustness”, *Applied Energy*, **226**, pp. 607-617, 2018.
[9] C. Saint-Martin et al., “Statistical performance assessment of a bistable vibration energy harvester”, *Mechanical Systems and Signal Processing*, *in press*.
[10] D. Hoffmann et al., “A self-adaptive energy harvesting system”, *Smart Materials and Structures*, **25**, 3, 035013, 2016.
[11] E.D. Niri and S. Salamone, “A passively tunable mechanism for a dual bimorph energy harvester with variable tip stiffness and axial load”, *Smart Materials and Structures*, **21**, 12, 125025, 2012.
[12] A. Brenes, A. Morel, J. Juillard, E. Lefeuvre, A. Badel, “Maximum power point of piezoelectric energy harvesters”, *Smart Materials and Structures*, **29**, 033001, 2020.
[13] W.-J. Wu, Y.-Y. Chen, B.-S. Lee, J.-J. He, Y.-T. Peng, “Tunable resonant frequency power harvesting devices”, *SPIE Smart Structures and Materials and Nondestructive Evaluation and Health Monitoring*, 61690A, 2006.
[14] Y. Liao, H. Sodano, “Optimal parameters and power characteristics of piezoelectric energy harvesters with an RC circuit”, *Smart Materials and Structures*, **18**, 045011, 2009.
[15] B. Ahmed-Seddik, G. Despesse, S. Boisseau and E. Defay, “Self-powered resonant frequency tuning for piezoelectric vibration energy harvesers”, *Journal of Physics: Conference Series (PowerMEMS),* **476**, 012069,

2013.
[16] A. Badel, E. Lefeuvre, "Wideband piezoelectric energy harvester tuned through its electronic interface circuit", *Journal of Physics: Conference Series (PowerMEMS),* **504**, 012115, 2014.
[17] A. Brenes, A. Morel, D. Gibus, C.-S. Yoo, P. Gasnier, E. Lefeuvre, A. Badel, "Large-bandwidth piezoelectric energy harvesting with frequency-tuning synchronized electric charge extraction", *Sensors and Actuators A: Physical*, **302**, 111759, 2020.
[18] A. Morel, G. Pillonnet, P. Gasnier, E. Lefeuvre, A. Badel «Frequency tuning of piezoelectric energy harvesters thanks to a short-circuit synchronous electric charge extraction», *Smart Materials and Structures*, **28**, 025009, 2018.
[19] P.H. Hsieh, C.H. Chen, H.C. Chen, «Improving the scavenged power of nonlinear piezoelectric energy harvesting interface at off-resonance by introducing switching delay», *IEEE Transactions on Power Electronics*, **30**, pp. 3142-3155, 2014.
[20] A. Morel, A. Quelen, C.A. Berlitz, D. Gibus, P. Gasnier, A. Badel, G. Pillonnet, «32.2 self-tunable phase-shifted SECE piezoelectric energy-harvesting ic with a 30nW mppt achieving 446% energy-bandwidth improvement and 94% efficiency», *IEEE International Solid-State Circuits Conference*, 488-490, 2020.
[21] Y. Cai, Y. Manoli, «A piezoelectric energy-harvesting interface circuit with fully autonomous conjugate impedance matching, 156% extended bandwidth, and 0.38 μW power consumption», *IEEE International Solid-State Circuits Conference*, 148-150, 2018.
[22] E. Lefeuvre, A. Badel, C. Richard. D. Guyomar, «Piezoelectric Energy Harvesting Device Optimization by Synchronous Electric Charge Extraction», *Journal of Intelligent Material Systems and Structures*, vol. 16, no. 10, pp. 865-876, 2005.
[23] Y. Wu, A. Badel, F. Formosa, W. Liu, A. E. Abgossou, «Piezoelectric vibration energy harvesting by optimized synchronous electric charge extraction», *Journal of Intelligent Material Systems and Structures*, vol. 24, no. 12, pp. 1445-1458, 2012.
[24] A. Richter, A. Strobel, N. Joram, F. Ellinger, L. Göpfert, and R. Marg, "Tunable interface for piezoelectric energy harvesting," in *2014 IEEE 11th International Multi-Conference on Systems, Signals Devices (SSD14)*, 2014, pp. 1–5.
[25] E. Lefeuvre, A. Badel, A. Brenes, S. Seok, and C.-S. Yoo, "Power and frequency bandwidth improvement of piezoelectric energy harvesting devices using phase-shifted synchronous electric charge extraction interface circuit," *Journal of Intelligent Material Systems and Structures*, vol. 28, no. 20, pp. 2988–2995, Dec. 2017.
[26] A. Morel, A. Badel, Y. Wanderoild, and G. Pillonnet, "A unified N-SECE strategy for highly coupled piezoelectric energy scavengers", *Smart Materials and Structures*, **27**, 084002, 2018.
[27] A. Erturk, D.J. Inman, "Issues in mathematical modeling of piezoelectric energy harvesters", *Smart Materials and Structures,* **17**, 065016, 2008.
[28] A. Morel, A. Brenes, D. Gibus, E. Lefeuvre, P. Gasnier, G. Pillonnet, and A. Badel, « A comparative study of electrical interfaces for tunable piezoelectric vibration energy harvesting", *Smart Materials and Structures*, **31**, 045016, 2022.
[29] Y. Liao, J. Liang, «Maximum power, optimal load, and impedance analysis of piezoelectric vibration energy harvesters», *Smart Materials and Structures*, **27**, 075053, 2018.
[30] Y. Liao, J. Liang, "Generalized modeling and analysis of piezoelectric vibration energy harvesters", Proc. SPIE 10967, Active and Passive Smart Structures and Integrated Systems XIII, 1096724 2019.
[31] A. Morel, A. Badel, R. Grézaud, P. Gasnier, G. Despesse, G. Pillonnet, "Resistive and reactive loads' influences on highly coupled piezoelectric generators for wideband vibrations energy harvesting", *Journal of Intelligent Material Systems and Structures* **30**, pp. 386-399, 2018.
[32] T. Teng-Tiow, I. Mareels, J. B. Moore, "High performance control", Chicago: *Birkhäuser*, pp. 93, 1998.
[33] W. Tian, Z. Zhao, W. Liu, Q. Zhu, Z. Zhang, Y. Yuan, «Analysis on the power and bandwidth improvement of a frequency-tuning optimized SECE circuit», *Sensors and Actuators A: Physical*, **332**, 113110, 2021.
[34] B. Zhao, J. Liang, K. Zhao, "Phase-variable control of parallel synchronized triple bias-flips interface circuit towards broadband piezoelectric energy harvesting", *2018 IEEE International Symposium on Circuits and Systems (ISCAS)*, pp. 1-5, 2018.
[35] A. Morel, R. Grézaud, G. Pillonnet, P. Gasnier, G. Despesse, and A. Badel, "Active AC/DC control for wideband piezoelectric energy harvesting," *J. Phys.: Conf. Ser.*, vol. 773, no. 1, p. 12059, 2016.